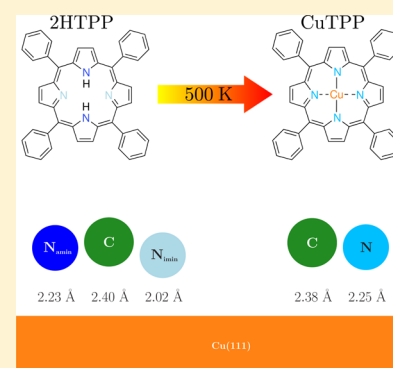


# Self-Metalation of 2*H*-Tetraphenylporphyrin on Cu(111) Studied with XSW: Influence of the Central Metal Atom on the Adsorption Distance

C. Bürker,<sup>†</sup> A. Franco-Cañellas,<sup>†</sup> K. Broch,<sup>†</sup> T.-L. Lee,<sup>‡</sup> A. Gerlach,<sup>\*,†</sup> and F. Schreiber<sup>†</sup><sup>†</sup>Institut für Angewandte Physik, Universität Tübingen, Auf der Morgenstelle 10, 72076 Tübingen, Germany<sup>‡</sup>Diamond Light Source, Harwell Science and Innovation Campus, Oxfordshire OX11 0DE, United Kingdom

## Supporting Information

**ABSTRACT:** We present a systematic X-ray standing wave (XSW) study of the  $\pi$ -conjugated organic compound 2*H*-tetraphenylporphyrin (2HTPP) and copper(II)-tetraphenylporphyrin (CuTPP) on Cu(111) at room and low temperatures. We exploit the feature of thermally activated self-metalation of 2HTPP to CuTPP to study the influence of the central metal atom on the bonding distance of the molecule to the substrate surface. Comparison between the average adsorption distances of the carbon and nitrogen atoms of 2HTPP reveals a distorted molecule with the nitrogen atoms being closer to the surface than the carbon ones on average. Additionally, the measured positions of the two chemically inequivalent types of nitrogen atoms (imino and amino) of 2HTPP indicate a distorted porphyrin ring. After the chemical reaction from 2HTPP to CuTPP at 500 K, no change of the adsorption distance of the carbon skeleton is seen, but the entire molecule becomes flattened. Despite the changes upon metalation, adsorption distances for both molecules show a strong interaction with the substrate in comparison to similar  $\pi$ -conjugated molecules.



## 1. INTRODUCTION

The investigation of large  $\pi$ -conjugated molecules has become an important field in surface science. To tailor the molecules and the metal in the desired way for an optimized functionality in organic devices, it is crucial to understand the phenomena occurring at the organic–metal interface.<sup>1–4</sup> Porphyrins are very promising compounds as they can be chemically modified to a large extent by attaching different side groups. For instance, the addition of four phenyl groups yields 2*H*-tetraphenylporphyrin (2HTPP, C<sub>44</sub>H<sub>30</sub>N<sub>4</sub>; see Figure 1 for the chemical structure), but also more complicated structures are possible. Additionally, the porphyrin macrocycle can host a metal atom, which adds further functionalities to the molecule. Thus, metaloporphyrins show sensing,<sup>5</sup> catalytic,<sup>6–8</sup> and optoelectronic properties,<sup>9–11</sup> as well as render an easy way to create tunable single metal–atom arrays.<sup>12–14</sup> Due to these promising features, the metalation of porphyrins has been widely studied in recent years. Allocation of metal atoms, deposited either before or after the porphyrins, and codeposition of both elements were first reported as suitable methods to study porphyrins and their metalated counterparts (see Panighel et al. and references therein<sup>15</sup> for different 2HTTP studies). Recently, González-Moreno et al.<sup>16</sup> first reported a different method to obtain metalated porphyrins, which consists in the thermally activated acquisition of the metal atom directly from the substrate. Since then, what is called “self-metalation” has been shown for different substrates, porphyrins, and temperatures.<sup>17–21</sup> For 2HTTP on Cu(111), Diller et al. first reported

the thermally activated self-metalation of 2HTPP to CuTPP + H<sub>2</sub>.<sup>22</sup> Different experimental techniques have been used to understand the process, which leads to changes in the geometric and electronic structure of this molecule.<sup>22,23</sup> In X-ray photoelectron spectroscopy (XPS), the N 1s core level of 2HTPP on Cu(111) consists of a double peak, which indicates that there are two different bonding mechanisms for the nitrogen atoms. The peak at higher binding energy is assigned to the two amino nitrogen atoms (–NH–, in the literature also assigned as the pyrrolic nitrogen), while the other peak corresponds to the imino nitrogen atoms (–N=).<sup>24</sup> Compared with a multilayer 2HTPP film, the binding energy of the imino nitrogen atoms in a monolayer on Cu(111) is lowered by 0.65 eV,<sup>25</sup> which is explained by strong interaction of the imino nitrogen atoms with the Cu(111) surface. After annealing to temperatures higher than 400 K, the XP spectrum of N 1s changes substantially,<sup>22</sup> and only the imino N 1s peak is visible.<sup>26</sup> This result is explained by self-metalation, that is, the formation of CuTPP,<sup>22</sup> which involves the removal of a H<sub>2</sub> molecule and causes all nitrogen atoms to be equally coordinated to the central metal atom. This means that it is possible by annealing to transform the metal-free TPP to a TPP with a central metal atom.

Received: April 1, 2014

Revised: May 22, 2014

Published: May 23, 2014

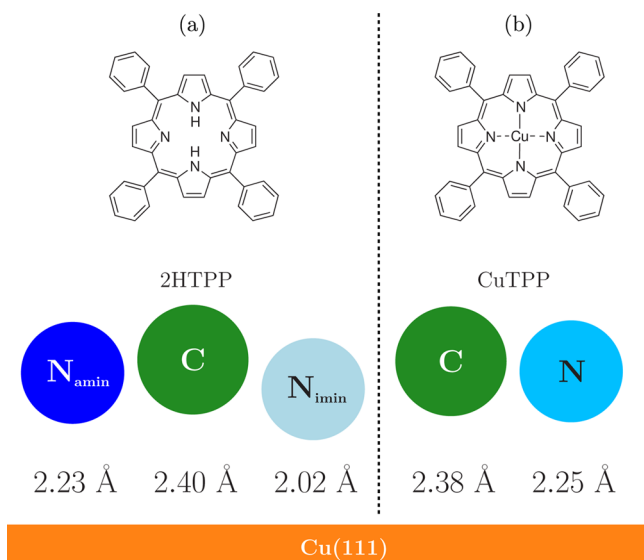


**Figure 1.** (a) Chemical structure of (a) 2HTPP and (b) CuTPP and the corresponding bonding distances on Cu(111). Note that, upon metalation, all nitrogen atoms are equally and indistinguishably coordinated to the copper atom.

Besides the electronic changes revealed by spectroscopic techniques, scanning tunnelling microscope (STM) pictures of 2HTPP and CuTPP on Cu(111) are also useful to detect other changes occurring upon heating to temperatures above 400 K.<sup>23</sup> For instance, at room temperature (RT), individual 2HTPP molecules can be imaged by STM due to the strong interaction of the iminic nitrogen atoms with the Cu(111) surface.<sup>23,25,27–30</sup> Interestingly, the same is not possible for low coverages of CuTPP due to its high mobility.<sup>23,27,28</sup> Instead, only at 200 K is the diffusion of the molecules slow enough to enable STM measurements.<sup>23</sup> However, for higher coverages, where CuTPP starts to aggregate, STM pictures can be recorded at RT.<sup>18,21,28</sup> Furthermore, STM results also show changes in the adsorption geometry of the molecule upon annealing. Thus, due to this strong interaction, 2HTPP molecules adsorb close to the surface following the high symmetry axis of the substrate and with the phenyl groups parallel to it.<sup>25,31</sup> Also, images show a distorted macrocycle due to the asymmetric interaction of the nitrogen atoms.<sup>23,27</sup> After annealing, the interaction decreases, and the phenyl groups in CuTPP are able to rotate with respect to the surface<sup>23</sup> (different conformations of the phenyl groups were also reported by near-edge X-ray absorption fine structure spectroscopy, NEXAFS<sup>22</sup>). These differences in STM images between 2HTPP and CuTPP were employed to study the metalation activation energy and reaction kinetics.<sup>27</sup> The orientation of the phenyl groups is also behind the different macromolecular arrangements of 2HTPP and CuTPP because T-type and  $\pi$ - $\pi$  stacking interactions<sup>32,33</sup> require a nonflat phenyl group that is not available for the nonmetalated porphyrin.<sup>30</sup>

In the last years, different techniques and simulation methods have been used to study the adsorption geometry and electronic properties of porphyrin derivatives on different substrates as well as their changes upon metalation. However, to the best of our knowledge, no direct attempt to measure the adsorption distances has been carried out so far. Self-metalation of 2HTPP on Cu(111) offers a relatively easy way to

systematically study, under different conditions, how the incorporation of a metal atom into the porphyrin ring affects the interaction strength with the surface. Results will provide, on one hand, further information on how metalation affects the geometry of the molecule, which is important to understand the supramolecular interactions and self-assembly properties of TPP,<sup>30,28</sup> and, on the other hand, with a more general perspective, the results will give a new insight into the influence of the central metal atom on the adsorption geometry of  $\pi$ -conjugated molecules on metal surfaces. To fill in this gap, we use the X-ray standing wave (XSW) technique to study 2HTPP and the self-metalated CuTPP on Cu(111) at different temperatures. In recent years, the XSW technique has demonstrated its potential to disentangle the complex bonding mechanism of large aromatic molecules on noble metal surfaces.<sup>34–41</sup> Details of the XSW technique can be found in refs 41–44.

## 2. EXPERIMENTAL DETAILS

The XSW and XPS experiments were performed at the beamline I09 of the Diamond Light Source (DLS) in Didcot, U.K. The end station in the experimental hutch 2 at I09 contains a load lock, a preparation chamber, and an analysis chamber. Each of them can be isolated by gate valves. A sketch of the setup is displayed in Figure 2. A five-axis ( $x$ ,  $y$ , and  $z$

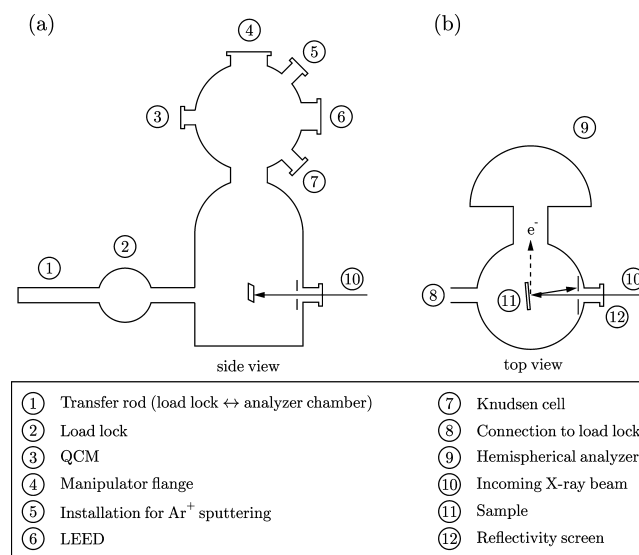


**Figure 2.** Schematic and simplified (a) side and (b) top view pictures of the setup in experimental hutch 2 at the DLS beamline I09. Not drawn are the pumping units of the chambers and the valves between the load lock, preparation, and analysis chambers.

translations and polar and azimuth rotations) manipulator is used for sample handling in the preparation chamber and for X-ray measurements in the analysis chamber. It is equipped with a sample heater capable of electron beam and resistive heating and a cooling system, which is operated with liquid nitrogen for the low-temperature (LT) measurements.

The preparation chamber features an ion gun for  $Ar^+$  sputtering, evaporator ports, a quartz crystal microbalance (QCM) on a linear translation, and a low-energy electron diffraction (LEED) system. The analysis chamber (base pressure,  $3 \times 10^{-10}$  mbar) contains a VG Scienta EW4000 HAXPES hemispherical electron analyzer, which is mounted at

$\sim 90^\circ$  relative to the incident X-ray beam. The acceptance angle of the electron analyzer is  $\pm 30^\circ$ .

Sample preparation and measurements took place in situ under ultrahigh vacuum conditions. The Cu(111) crystal (MaTecK) was cleaned by repeated cycles of Ar<sup>+</sup> sputtering and annealing to 800 K. The surface cleanliness was checked with XPS and LEED. 2HTPP was purchased from Sigma-Aldrich (purity  $\geq 99\%$ ) and degassed thoroughly. Submonolayer films were prepared by organic molecular beam deposition using a homemade Knudsen cell, and the evaporation rate was monitored using the available QCM. A typical nominal deposition rate was  $\sim 0.2 \text{ \AA}/\text{min}$ . The final molecular coverage, being  $\sim 0.3 \text{ ML}$ , was calculated using the intensity ratio of the cross section corrected C 1s to Cu 3p<sub>3/2</sub> core levels and the size of the unit cell occupied by a TPP molecule. CuTPP was obtained upon annealing of the 2HTPP samples to 500 K for 2 min.

The overall energy resolution for the photon energies that we worked at was about 350 meV, being dominated by the resolution of the Si(111) double-crystal monochromator. The X-ray beam at the sample was defocused to a size of approximately  $300 \times 300 \mu\text{m}^2$ .

XPS measurements were performed at RT and LT at photon energies  $\sim 5 \text{ eV}$  above the Bragg energy of Cu(111), which was for our geometry  $E_{\text{Bragg}}^{\text{RT}} = 2.973 \text{ keV}$  and  $E_{\text{Bragg}}^{\text{LT}} = 2.980 \text{ keV}$ . The difference between the Bragg energies was used to determine the LT, that is, 146 K, based on the known thermal expansion of copper.<sup>45</sup>

For the XSW measurements, the photon energy was scanned around the first-order Bragg reflection of the Cu(111) substrate. The result of the XSW analysis is given by two fitting parameters, that is, the coherent position  $P_{\text{H}}$  and the coherent fraction  $f_{\text{H}}$ . The first can be related to the bonding distance  $d_{\text{H}}$  via  $d_{\text{H}} = (n + P_{\text{H}})d_0$ . Here,  $d_0$  is the lattice spacing of the (111) Bragg reflection, and  $n$  is a non-negative integer. The latter varies within the range of  $0 \leq f_{\text{H}} \leq 1$  and reflects the degree of vertical order.  $f_{\text{H}} = 1$  means perfect order (all atoms of the analyzed chemical species have the same distance to the topmost surface plane), whereas  $f_{\text{H}} = 0$  stands for a disordered layer (random distances to the surface).

### 3. RESULTS AND ANALYSIS

**3.1. Photoemission Analysis.** The XPS analysis of the N 1s and C 1s core-level signals of TPP on Cu(111) is displayed in Figures 3 and 4, respectively, which are arranged as follows: The uppermost spectra were recorded on a fresh spot on the sample (labeled “before XSW scan”), the central spectra were taken after a XSW measurement (“after XSW scan”), and the bottom panels show spectra measured after annealing to 500 K. Each spectrum is background-subtracted (Shirley background for the C 1s and linear background for the N 1s) and fitted with two Gaussians.

**3.1.1. XPS Analysis of the N 1s Signal.** As reported in previous studies,<sup>21–25,28</sup> the N 1s signal consists of two contributions, one from the aminic and the other from the iminic nitrogen atoms. The latter interacts more strongly with the copper atoms in the substrate surface. The expected intensity ratio of the two contributions is 1:1, but we measured a weaker aminic component and noticed a continuous change of the intensity ratio due to exposure to X-ray radiation, causing the aminic component to diminish and the iminic component to grow, as can be clearly seen in Figure 3 at both RT and LT, although the total N 1s intensity was found to stay constant.

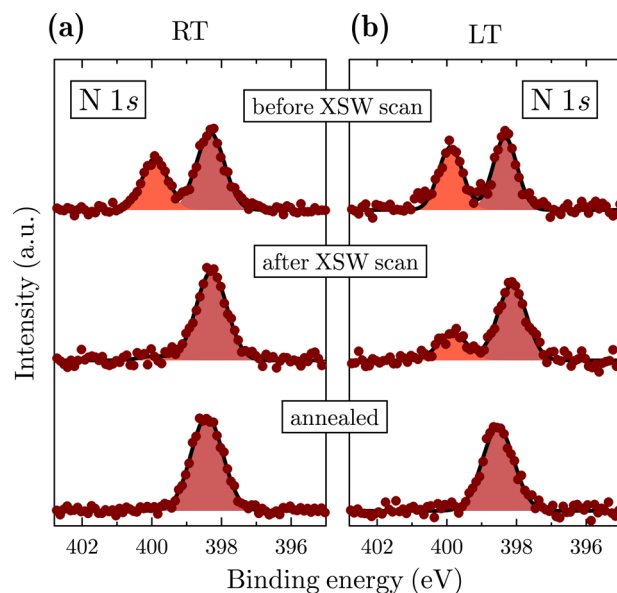


**Figure 3.** XPS analysis of the N 1s core-level signal of 2HTPP on Cu(111). We observed spectral changes for the N 1s signal due to synchrotron radiation. Therefore, spectra are shown for a fresh spot (“before XSW scan”), for a spot exposed to X-rays (“after XSW scan”), and for the annealed sample, both for RT and for LT.

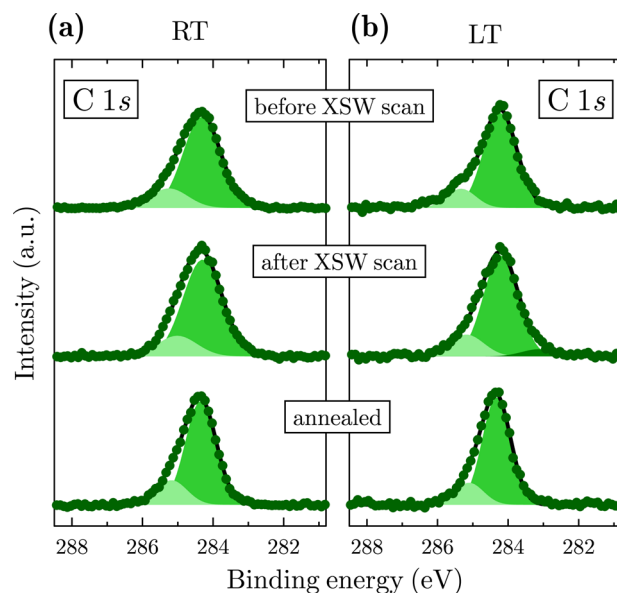


**Figure 4.** XPS analysis of the C 1s core-level signal of 2HTPP on Cu(111). Spectra are shown for a fresh spot (“before XSW scan”), for a spot exposed to X-rays (“after XSW scan”), and for the annealed sample, both for RT and for LT. No substantial change in the C 1s spectra indicates that the molecule stays intact upon X-ray illumination. The vanishing peak correlated with the aminic nitrogen atoms can be explained by the metalation of the 2HTPP molecule to CuTPP induced by X-rays.

Note that the two spectra in the middle were taken after different X-ray exposures. Therefore, the difference in height of the aminic peak is not due to the different sample temperatures but rather due to different irradiation times. Upon heating the sample to 500 K, only one nitrogen peak remained, which was used as a fingerprint for metalation.<sup>22,23,28</sup> As an additional test for the metalation process, thermal desorption measurements were performed in our home laboratory, which, indeed, confirm

the existence of CuTPP after annealing (see the Supporting Information (SI)<sup>46</sup>).

Our measured binding energies for the iminic and aminic nitrogen atoms stay constant within the error bars ( $\pm 350$  meV), 398.3 and 399.9 eV, respectively. They are in good agreement with previously determined binding energies.<sup>22,23,28</sup> No noticeable change in binding energy is observed upon cooling or annealing. All binding energies are summarized in Table 1. Similarly, no variation beyond our error bars is found for the widths (fwhm) of the individual N 1s peaks, being around 0.9 eV.

**Table 1. Binding Energies for the C 1s and N 1s Core-Level Signal of TPP on Cu(111) for Different Situations<sup>a</sup>**

	RT			LT		
	before	after	annealed	before	after	annealed
N 1s (iminic) <sup>26</sup>	398.3	398.3	398.4	398.3	398.2	398.5
N 1s (aminic)	399.9	399.9		399.9	399.8	
C 1s (C <sup>C</sup> )	284.3	284.3	284.4	284.2	284.2	284.3
C 1s (C <sup>N</sup> )	285.3	285.0	285.2	285.4	285.2	285.1

<sup>a</sup>The binding energies were measured on a fresh spot (labeled “before”), after a XSW measurement (labeled “after”), and for the annealed sample. All values are in units of eV.

**3.1.2. XPS Analysis of the C 1s Signal.** The asymmetric shape of all C 1s signals is fitted using two Gaussians with identical width. The higher binding energy component originates from the eight carbon atoms that form bonds with the nitrogen, while the lower binding energy one accounts for those (36 carbon atoms) forming bonds with other carbon and/or hydrogen atoms. For all sample conditions (RT, LT, and annealed), the intensity ratio of the two peaks,  $I(\text{C}-\text{C})/I(\text{C}-\text{N})$  agrees with the expected value of 4.5 (36/8) within a variation of  $\pm 0.2$ .

The binding energy of the stronger component (carbon surrounded by other carbon) is 284.3 eV. The weaker component (carbon atoms bound to also nitrogen atoms) is found to be at a binding energy of 285.2 eV. The width of the peaks changes only slightly. The fwhm is found to be 1.3, 1.1, and 1.0 eV for 2HTPP/CuTPP measured at LT, RT, and the annealed sample, respectively. All binding energies are summarized in Table 1.

**3.2. XSW Analysis.** **3.2.1. Corrections of XSW Measurements of 2HTPP on Cu(111).** The change of the N 1s spectra upon thermal annealing to 500 K has been explained by self-metalation of the 2HTPP molecule forming CuTPP.<sup>21–23</sup> Here, we observed a similar behavior induced by X-rays of 2.98 keV. The fact that the C 1s signal does not change during X-ray exposure supports the idea of a beam-induced chemical reaction from 2HTPP to CuTPP and rules out beam damage as the cause of the nitrogen core-level changes because in the latter case, the molecules would have been destroyed upon X-ray illumination.

As this chemical reaction changes the intensities of the two N 1s components, the XSW-modulated photoelectron yields are affected. To account for the changing XPS intensities due to this beam-induced chemical reaction, we applied a correction to the yield curves. The XP spectrum before and after a XSW scan and the time between the two spectra were used to determine the reaction rate.<sup>46</sup> A linear slope with a gradient corresponding to the reaction rate was assumed and subtracted from the iminic photoelectron yield and added to the aminic one. The

result of this correction can be seen in Figure 5. The uncorrected yield curves are displayed in Figure 5a, where

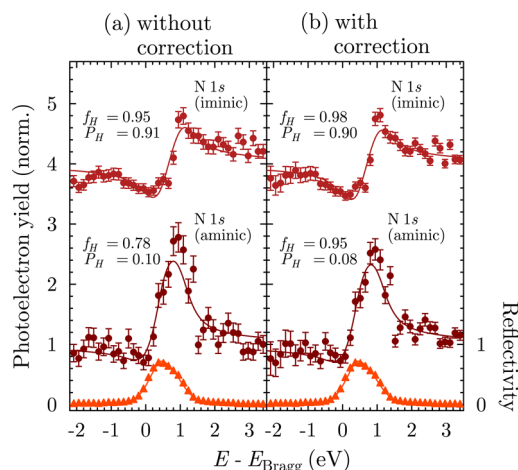


**Figure 5.** Example of XSW measurement with reflectivity (triangles) and photoelectron yield curves (circles) of 2HTPP on Cu(111) with the fitting parameters  $f_H$  and  $P_H$  for the yield curves of the N 1s signal, measured at LT. (a) Not corrected yield curves for the aminic and iminic nitrogen atoms. (b) A linear correction was added (subtracted) to the yield curves of the aminic (iminic) nitrogen atoms in order to account for the metalation of 2HTPP upon X-ray illumination.

the measured iminic N 1s yields are mostly below (above) the best fit at the start (end) of the scan, which is on the left (right) side of the plot. The opposite can be observed for the yield curve of the aminic nitrogen. Figure 5b displays the corrected yield curves, where one can see a better agreement with the best fit due to the correction. This correction leads to changes of the coherent positions of the order of  $\Delta P_H \leq 0.02$  and coherent fractions of  $\Delta f_H \leq 0.2$ .

**3.2.2. XSW Measurements of 2HTPP on Cu(111).** Several XSW measurements were performed for the C 1s and N 1s core levels at RT and LT. All aminic and iminic N 1s photoelectron yields were corrected as described in the previous section. Note that the tabulated results given below refer to the average over all individual measurements for each species, while in Figures 6 and 7, single XSW measurements are shown as an example.

At RT, the analysis of the N 1s photoelectron yield reveals for the aminic nitrogen atoms a bonding distance to the Cu(111) surface of 2.23 Å, and for the iminic nitrogen, the distance is 2.02 Å. The average carbon bonding distance is 2.40 Å. At LT, small changes are observed for the aminic nitrogen atoms (2.28 Å), the iminic nitrogen atoms (1.97 Å), and the carbon atoms (2.34 Å). All results are summarized in Table 2.

**3.2.3. XSW Measurements of CuTPP on Cu(111).** After annealing the sample to 500 K, 2HTPP was transformed to CuTPP.<sup>21–23</sup> Several XSW measurements were performed for the new system at RT and LT. The carbon atoms were found to adsorb on average at a distance of 2.38 (RT) and 2.33 Å (LT) to the Cu(111) surface. The average distance for the nitrogen atoms was determined to be 2.25 Å at both RT and LT. All results of the annealed sample are summarized in Table 3.

## 4. DISCUSSION

Our XPS results are consistent with previous results.<sup>22,23,28</sup> Measuring nitrogen core levels before and after the metalation represents a direct, noninvasive method to monitor the

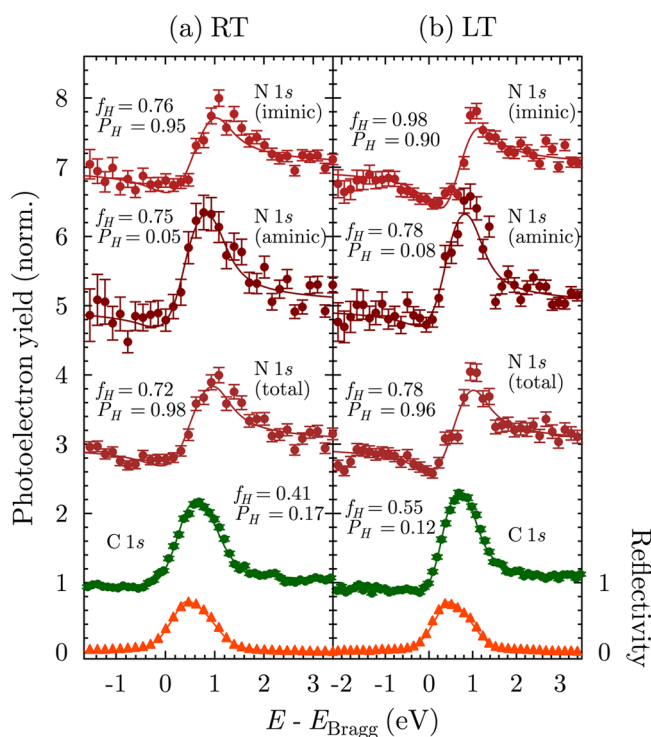


**Figure 6.** Example of XSW measurement with reflectivity (triangles) and photoelectron yield curves (circles) of 2HTPP on Cu(111) with the fitting parameters  $f_H$  and  $P_H$  for the yield curves of the C 1s and N 1s signals at RT and LT. The N 1s yield curves of the aminic and iminic nitrogen atoms are corrected as described in section 3.2.1.

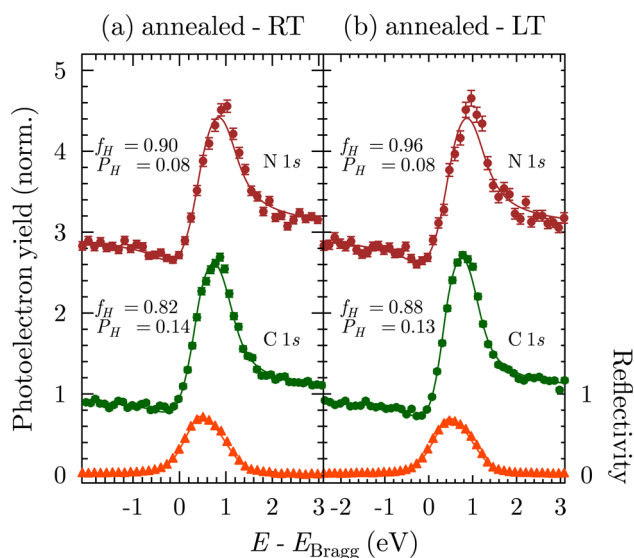


**Figure 7.** Example of XSW measurement with reflectivity (triangles) and photoelectron yield curves (circles) of CuTPP on Cu(111) with the fitting parameters  $f_H$  and  $P_H$  for the yield curves of the C 1s and N 1s signals at RT and LT.

reaction, that is, the two different nitrogen peaks for 2HTPP (corresponding to different bonding environments) becoming one single peak upon metalation (due to the identical coordination to the incorporated copper atom). Moreover, the formation of CuTPP was checked by thermal desorption spectroscopy,<sup>46</sup> giving direct evidence of the existence of this molecule upon annealing.

As expected, the two types of nitrogen atoms for 2HTPP, the aminic (with a N–H bond) and the iminic (–N=), adsorb at different distances to the Cu(111) surface. At RT, the rather small bonding distance of the iminic nitrogen (2.02 Å) supports the earlier finding of a strong interaction between nitrogen and the substrate.<sup>22,25,47</sup> The bonding distance of the aminic nitrogen atom is  $\sim 0.2$  Å larger (2.23 Å). These different distances signify a saddle shape of the porphyrin ring, as suggested before<sup>23,25,47</sup> and in accordance with NEXAFS<sup>22</sup> results of 2HTPP on Cu(111) and by density functional theory (DFT) calculations for the reaction of porphyrin with single metal atoms, including Cu.<sup>24</sup>

The average distance of the carbon atoms of 2HTPP (2.40 Å at RT) suggests that the phenyl groups, which can rotate around the axis of the bond to the porphyrin core, adsorb rather parallel to the surface. Another finding that supports this statement is the relatively high coherent fraction for the carbon atoms, which clearly indicates an essentially flat-lying molecule, including its phenyl groups. This finding is in line with other experimental results. NEXAFS measurements<sup>22</sup> determined a rotation of the phenyl groups of 20°, whereas it was estimated to be 10° based on STM measurements.<sup>47</sup>

Upon annealing of 2HTPP and the consequential induced chemical reaction to CuTPP, a change in the adsorption distance of the nitrogen atoms was observed. Thus, the equal coordination of all nitrogen atoms to the central Cu atom eliminates the iminic and aminic differences, resulting in one single bonding distance of 2.25 Å to the Cu(111) surface. This distance is 0.1 Å higher than the average adsorption distance of nitrogen atoms in 2HTPP (2.15 Å). Metalation also increases the coherent fraction for both nitrogen and carbon atoms. The explanation of these results is that the incorporation of the Cu atom relaxes the geometry of the porphyrin ring, that is, the suppression of the strong iminic–substrate interaction turns the saddle shape conformation into a relatively flat macrocycle, which is supported by the increase of the coherent fractions (compare  $f_H$  for N 1s in Tables 2 and 3) and also found by independent NEXAFS measurements.<sup>22</sup> The suppression of the site-specific interaction of the iminic nitrogen with the substrate together with the relaxation and lifting of nitrogen atoms upon metalation explains the STM results that show a higher mobility of CuTPP in comparison to that of 2HTPP.<sup>23,27,28</sup>

Despite the changes in the nitrogen adsorption, the average distance of the carbon atoms remains basically unaffected (2.40 versus 2.38 Å at RT) after the chemical reaction at 500 K. A similar behavior was seen in a STM study of metalation at different temperatures carried out by Xiao et al.<sup>23</sup> They observed a temperature-dependent rotation of the phenyl groups that affected the adsorption behavior of the molecule. Particularly, their images of CuTPP obtained after annealing at 500 K showed a molecular arrangement similar to that of nonmetalated 2HTPP, that is, with the phenyl groups lying parallel to the Cu substrate, rendering a flat molecule. It is suggested that this flattening of the phenyl groups upon annealing to higher temperatures happens due to the dehydrogenation of the phenyl groups and/or the macrocycle. This dehydrogenation reduces the steric repulsion between the center ring and the side groups, allowing a more planar conformation of the whole molecule.<sup>48</sup>

Because our measurements are performed on molecules that both have the phenyl groups rather parallel to the substrate, we can neglect a possible rotation as a contribution to the adsorption height. Hence, the XSW results only reveal the

Table 2. XSW Results (Coherent Fraction, Coherent Position, Bonding Distance) of 2HTPP on Cu(111) at RT and LT<sup>a</sup>

	RT			LT		
	$f_H$	$P_H$	$d_H$ (Å)	$f_H$	$P_H$	$d_H$ (Å)
N 1s (iminic)	0.67	0.97	$2.02 \pm 0.08$	0.84	0.94	$1.97 \pm 0.08$
N 1s (aminic)	0.72	0.07	$2.23 \pm 0.05$	0.85	0.09	$2.28 \pm 0.05$
N 1s (total)	0.61	0.03	$2.15 \pm 0.08$	0.70	0.98	$2.04 \pm 0.06$
C 1s (total)	0.52	0.15	$2.40 \pm 0.03$	0.65	0.12	$2.34 \pm 0.02$

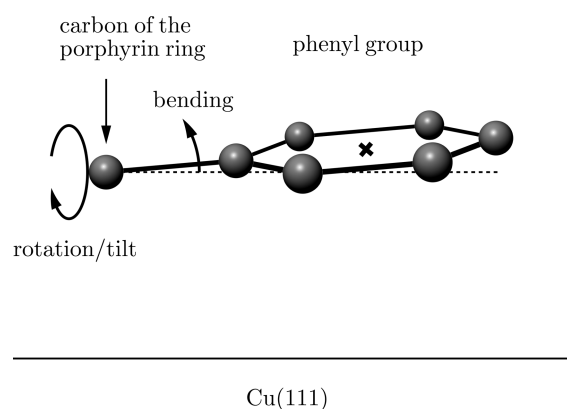
<sup>a</sup>The results of the aminic and iminic nitrogen atoms were obtained performing the correction method described earlier.

Table 3. XSW Results (Coherent Fraction, Coherent Position, Bonding Distance) of CuTPP on Cu(111) at RT and LT

	RT			LT		
	$f_H$	$P_H$	$d_H$ (Å)	$f_H$	$P_H$	$d_H$ (Å)
N 1s	0.90	0.08	$2.25 \pm 0.02$	0.93	0.08	$2.25 \pm 0.02$
C 1s (total)	0.71	0.14	$2.38 \pm 0.02$	0.84	0.12	$2.33 \pm 0.02$

influence of the nitrogen–substrate interaction, which, as we see, does not have a major effect on the average adsorption height of carbon atoms. However, after annealing to 500 K, the vertical order is clearly affected, as shown by the increase of the coherent fractions for both the carbon and the nitrogen atoms (compare  $f_H$  before metalation in Table 2 and afterward in Table 3). Therefore, metalation relaxes and flattens the macrocycle, but it is the rotation of the phenyl groups that is the main parameter that affects the adsorption distance to the substrate.

It is interesting to note that, although the molecule is flattened, the difference between the adsorption heights of carbon (2.38 Å at RT) and nitrogen (2.25 Å at RT) still represents a distorted molecule. From NEXAFS<sup>22</sup> measurements and STM images,<sup>23</sup> it is plausible to assume a completely flat macrocycle, that is, that the carbon atoms of the porphyrin ring are adsorbed at the same distance as the nitrogen ones (2.25 Å). In this case, the difference between nitrogen and carbon must be based on a larger average distance of the phenyl groups compared to the carbons of the macrocycle. A larger average distance to the surface can be achieved by an upward bending of the phenyl groups, as depicted in Figure 8. To obtain the experimentally determined mean carbon distances of 2.38 Å, the average distance of the phenyl groups (marked by a cross in Figure 8) to the surface has to be 2.48 Å. This value is



**Figure 8.** Schematic picture of a phenyl group showing the bending angle away from the surface. For CuTPP, the bending angle is  $\sim 5^\circ$ , and the corresponding mean distance of the side group (marked by a cross) is 2.48 Å, independent of the rotation (which here is arbitrarily chosen for a better depiction).

consistent with an upward bending of the phenyl groups of  $\sim 5^\circ$ ,<sup>46</sup> which is compatible and independent of any rotation of the entire group.

The same reasoning can be applied to the nonmetalated 2HTTP if we assume that for the saddle-shaped macrocycle carbon atoms are adsorbed at the mean distance between the aminic and iminic nitrogen (i.e., at  $\sim 2.13$  Å). In this case, to account for the average distance of 2.40 Å for carbon, the center of the phenyl group (the cross in Figure 8) has to be at 2.63 Å. This leads to a bending of the side groups of  $\sim 10^\circ$ .<sup>46</sup>

The reduction in the bending of the phenyl groups upon annealing (from 10 to  $5^\circ$ ) is possibly explained by the same reason as the flattening of the phenyl groups upon annealing, that is, the reduction of the steric repulsion between the side groups and the porphyrin macrocycle due to the dehydrogenation of both upon annealing at 500 K.<sup>48</sup> This reduction of the bending of the side groups also contributes to the increase of the coherent fraction upon metalation.

The adsorption scenario discussed above is qualitatively the same for both RT and LT. The lower adsorption heights as well as the higher coherent fractions observed at LT are most likely due to a smaller vibrational amplitude, as observed before in XSW studies at different temperatures (see, e.g., refs 49 and 50). At LT, the calculated bendings of the phenyl groups are  $8^\circ$  for 2HTTP and  $3^\circ$  for CuTPP.

One may compare the CuTPP molecule with Cu-phthalocyanine (CuPc) on Cu(111), which has been studied by XSW in great detail at different submonolayer coverages and temperatures (300 and 183 K).<sup>51</sup> It is found that CuPc on Cu(111) does not show a temperature-dependent adsorption distance, in line with our results of CuTPP. Instead, for CuPc on Cu(111), a dependence on the coverage was reported. Therefore, we compare our values with the results for 0.4 ML of CuPc, which is close to our coverage of CuTPP. The distance to the Cu(111) surface for CuPc ( $d_H(C) = 2.64$  Å and  $d_H(N) = 2.54$  Å) is larger than that for CuTPP, where the  $d_H(C) = 2.38$  Å, and  $d_H(N) = 2.25$  Å. Qualitatively, the two molecules adsorb in a similar way on the Cu(111) surface, with the nitrogen atoms at shorter distances to the surface. Yet, the CuTPP molecule is by almost 0.3 Å considerably closer to the surface and therefore interacting stronger with the surface than CuPc.

## 5. CONCLUSION

In conclusion, we find evidence of a strong interaction for both the metal-free and the metalated TPP molecules with the Cu(111) substrate in comparison to similar  $\pi$ -conjugated organic molecules. The distance of the carbon atoms to the Cu(111) surface before and after the metalation is very similar, showing a flat-lying molecule. This similarity goes against the effect of the strong iminic nitrogen–substrate interaction as the origin of the strong interaction. For 2HTPP, the bonding distance of the two types of nitrogen atoms reveals a distorted porphyrin ring toward a saddle shape, which becomes flat upon metalation as all four nitrogen atoms are now equally coordinated to the central Cu atom. From the measurements, we also estimate a small bending angle of the phenyl groups away from the surface that is reduced upon metalation. Neither for 2HTPP nor for CuTPP did we observe temperature-induced changes in the adsorption. Besides the thermally activated self-metalation, we detect a self-metalation induced by hard X-rays.

## ■ ASSOCIATED CONTENT

### Supporting Information

Thermal desorption spectrum of a CuTPP monolayer, hard X-ray photoelectron yield for the iminic and aminic nitrogen peaks of 2HTPP, calculation of the bending angle, and sketch of the phenyl group and its bond to the porphyrin ring. This material is available free of charge via the Internet at <http://pubs.acs.org>.

## ■ AUTHOR INFORMATION

### Corresponding Author

\*E-mail: [alexander.gerlach@uni-tuebingen.de](mailto:alexander.gerlach@uni-tuebingen.de).

### Notes

The authors declare no competing financial interest.

## ■ ACKNOWLEDGMENTS

This work was carried out with the support of the Diamond Light Source. This work was financially supported by the DFG (SCHR700/14-1).

## ■ REFERENCES

- (1) Heimel, G.; Duhm, S.; Salzmann, I.; Gerlach, A.; Strozecka, A.; Niederhausen, J.; Bürker, C.; Hosokai, T.; Fernandez-Torrente, I.; Schulze, G.; et al. Charged and Metallic Molecular Monolayers through Surface-Induced Aromatic Stabilization. *Nat. Chem.* **2013**, *5*, 187–194.
- (2) Stadler, C.; Hansen, S.; Kröger, I.; Kumpf, C.; Umbach, E. Tuning Intermolecular Interaction in Long-Range-Ordered Submonolayer Organic Films. *Nat. Phys.* **2009**, *5*, 153–158.
- (3) Koch, N.; Gerlach, A.; Duhm, S.; Glowatzki, H.; Heimel, G.; Vollmer, A.; Sakamoto, Y.; Suzuki, T.; Zegenhagen, J.; Rabe, J. P.; et al. Adsorption Induced Intramolecular Dipole: Correlating Molecular Conformation and Interface Electronic Structure. *J. Am. Chem. Soc.* **2008**, *130*, 7300–7304.
- (4) Yamane, H.; Gerlach, A.; Duhm, S.; Tanaka, Y.; Hosokai, T.; Mi, Y. Y.; Zegenhagen, J.; Koch, N.; Seki, K.; Schreiber, F. Site-Specific Geometric and Electronic Relaxations at Organic–Metal Interfaces. *Phys. Rev. Lett.* **2010**, *105*, 046103/1–046103/4.
- (5) Rakow, N. A.; Suslick, K. S. A Colorimetric Sensor Array for Odour Visualization. *Nature* **2000**, *406*, 710–713.
- (6) Meunier, B. Metalloporphyrins as Versatile Catalysts for Oxidation Reactions and Oxidative DNA Cleavage. *Chem. Rev.* **1992**, *92*, 1411–1456.

(7) Bhugun, I.; Lexa, D.; Savéant, J.-M. Homogeneous Catalysis of Electrochemical Hydrogen Evolution by Iron(0) Porphyrins. *J. Am. Chem. Soc.* **1996**, *118*, 3982–3983.

(8) Hulsken, B.; Van Hameren, R.; Gerritsen, J. W.; Khoury, T.; Thordarson, P.; Crossley, M. J.; Rowan, A. E.; Nolte, R. J. M.; Elemans, J. A. A. W.; Speller, S. Real-Time Single-Molecule Imaging of Oxidation Catalysis at a Liquid–Solid Interface. *Nat. Nanotechnol.* **2007**, *2*, 285–289.

(9) Baldo, M. A.; O'Brien, D. F.; You, Y.; Shoustikov, A.; Sibley, S.; Thompson, M. E.; Forrest, S. R. Highly Efficient Phosphorescent Emission from Organic Electroluminescent Devices. *Nature* **1998**, *395*, 151–154.

(10) Imahori, H.; Fukuzumi, S. Porphyrin- and Fullerene-Based Molecular Photovoltaic Devices. *Adv. Funct. Mater.* **2004**, *14*, 525–536.

(11) Koiry, S.; Jha, P.; Aswal, D.; Nayak, S.; Majumdar, C.; Chattopadhyay, S.; Gupta, S.; Yakhmi, J. Diodes Based on Bilayers Comprising of Tetrphenyl Porphyrin Derivative and Fullerene for Hybrid Nanoelectronics. *Chem. Phys. Lett.* **2010**, *485*, 137–141.

(12) Scheybal, A.; Ramsvik, T.; Bertschinger, R.; Putero, M.; Nolting, F.; Jung, T. Induced Magnetic Ordering in a Molecular Monolayer. *Chem. Phys. Lett.* **2005**, *411*, 214–220.

(13) Wende, H.; Bernien, M.; Luo, J.; Sorg, C.; Ponpandian, N.; Kurde, J.; Miguel, J.; Piantek, M.; Xu, X.; Eckhold, P.; et al. Substrate-Induced Magnetic Ordering and Switching of Iron Porphyrin Molecules. *Nat. Mater.* **2007**, *6*, 516–520.

(14) Wäckerlin, C.; Chylarecka, D.; Kleibert, A.; Müller, K.; Iacovita, C.; Nolting, F.; Jung, T. A.; Ballav, N. Controlling Spins in Adsorbed Molecules by a Chemical Switch. *Nat. Commun.* **2010**, *1*, 1–7.

(15) Panighel, M.; Di Santo, G.; Caputo, M.; Lal, C.; Taleatu, B.; Goldoni, A. Review of 2H-Tetrphenylporphyrins Metalation in Ultra-High Vacuum on Metal Surfaces. *J. Phys.: Conf. Ser.* **2013**, *470*, 012012/1–012012/6.

(16) González-Moreno, R.; Sánchez-Sánchez, C.; Trelka, M.; Otero, R.; Cossaro, A.; Verdini, A.; Floreano, L.; Ruiz-Bermejo, M.; García-Lekue, A.; Martín-Gago, J. A.; et al. Following the Metalation Process of Protoporphyrin IX with Metal Substrate Atoms at Room Temperature. *J. Phys. Chem. C* **2011**, *115*, 6849–6854.

(17) Doyle, C. M.; Krasnikov, S. A.; Sergeeva, N. N.; Preobrajenski, A. B.; Vinogradov, N. A.; Sergeeva, Y. N.; Senge, M. O.; Cafolla, A. A. Evidence for the Formation of an Intermediate Complex in the Direct Metalation of Tetra(4-bromophenyl)-porphyrin on the Cu(111) Surface. *Chem. Commun.* **2011**, *47*, 12134–12136.

(18) Haq, S.; Hanke, F.; Dyer, M. S.; Persson, M.; Iavicoli, P.; Amabilino, D. B.; Raval, R. Clean Coupling of Unfunctionalized Porphyrins at Surfaces to Give Highly Oriented Organometallic Oligomers. *J. Am. Chem. Soc.* **2011**, *133*, 12031–12039.

(19) Goldoni, A.; Pignedoli, C. A.; Di Santo, G.; Castellarin-Cudia, C.; Magnano, E.; Bondino, F.; Verdini, A.; Passerone, D. Room Temperature Metalation of 2H-TPP Monolayer on Iron and Nickel Surfaces by Picking up Substrate Metal Atoms. *ACS Nano* **2012**, *6*, 10800–10807.

(20) Diller, K.; Klappenberger, F.; Allegretti, F.; Papageorgiou, A. C.; Fischer, S.; Wiengarten, A.; Joshi, S.; Seufert, K.; Écija, D.; Auwärter, W.; et al. Investigating the Molecule-Substrate Interaction of Prototypic Tetrapyrrole Compounds: Adsorption and Self-Metalation of Porphine on Cu(111). *J. Chem. Phys.* **2013**, *138*, 154710 1–9.

(21) Nowakowski, J.; Wäckerlin, C.; Girovsky, J.; Siewert, D.; Jung, T. A.; Ballav, N. Porphyrin Metalation Providing an Example of a Redox Reaction Facilitated by a Surface Reconstruction. *Chem. Commun.* **2013**, *49*, 2347–2349.

(22) Diller, K.; Klappenberger, F.; Marschall, M.; Hermann, K.; Nefedov, A.; Wöll, C.; Barth, J. V. Self-Metalation of 2H-Tetrphenylporphyrin on Cu(111): An X-ray Spectroscopy Study. *J. Chem. Phys.* **2012**, *136*, 014705/1–014705/13.

(23) Xiao, J.; Ditzel, S.; Chen, M.; Buchner, F.; Stark, M.; Drost, M.; Steinrück, H.-P.; Gottfried, J. M.; Marbach, H. Temperature-Dependent Chemical and Structural Transformations from 2H-

Tetraphenylporphyrin to Copper(II)-Tetraphenylporphyrin on Cu(111). *J. Phys. Chem. C* **2012**, *116*, 12275–12282.

(24) Shubina, T. E.; Marbach, H.; Flechtner, K.; Kretschmann, A.; Jux, N.; Buchner, F.; Steinrück, H.-P.; Clark, T.; Gottfried, J. M. Principle and Mechanism of Direct Porphyrin Metalation: Joint Experimental and Theoretical Investigation. *J. Am. Chem. Soc.* **2007**, *129*, 9476–9483.

(25) Buchner, F.; Xiao, J.; Zillner, E.; Chen, M.; Röckert, M.; Ditzte, S.; Stark, M.; Steinrück, H.-P.; Gottfried, J. M.; Marbach, H. Diffusion, Rotation, and Surface Chemical Bond of Individual 2H-Tetraphenylporphyrin Molecules on Cu(111). *J. Phys. Chem. C* **2011**, *115*, 24172–24177.

(26) Upon metalation, the remaining N 1s peak has a binding energy slightly shifted with respect to the nonmetalated iminic peak. However, for simplicity, we refer to those nitrogen atoms equally coordinated to the central Cu atom, which yield the single N 1s XPS peak, as *iminic* as well.

(27) Ditzte, S.; Stark, M.; Drost, M.; Buchner, F.; Steinrück, H.-P.; Marbach, H. Activation Energy for the Self-Metalation Reaction of 2H-Tetraphenylporphyrin on Cu(111). *Angew. Chem., Int. Ed.* **2012**, *51*, 10898–10901.

(28) Röckert, M.; Ditzte, S.; Stark, M.; Xiao, J.; Steinrück, H.-P.; Marbach, H.; Lytken, O. Abrupt Coverage-Induced Enhancement of the Self-Metalation of Tetraphenylporphyrin with Cu(111). *J. Phys. Chem. C* **2014**, *118*, 1661–1667.

(29) Rojas, G.; Simpson, S.; Chen, X.; Kunkel, D. A.; Nitz, J.; Xiao, J.; Dowben, P. A.; Zurek, E.; Enders, A. Surface State Engineering of Molecule–Molecule Interactions. *Phys. Chem. Chem. Phys.* **2012**, *14*, 4971–4976.

(30) Stark, M.; Ditzte, S.; Drost, M.; Buchner, F.; Steinrück, H.-P.; Marbach, H. Coverage Dependent Disorder–Order Transition of 2H-Tetraphenylporphyrin on Cu(111). *Langmuir* **2013**, *29*, 4104–4110.

(31) Rojas, G.; Chen, X.; Bravo, C.; Kim, J.-H.; Kim, J.-S.; Xiao, J.; Dowben, P. A.; Gao, Y.; Zeng, X. C.; Choe, W.; et al. Self-Assembly and Properties of Nonmetalated Tetraphenyl-Porphyrin on Metal Substrates. *J. Phys. Chem. C* **2010**, *114*, 9408–9415.

(32) Brede, J.; Linares, M.; Kuck, S.; Schwbel, J.; Scarfato, A.; Chang, S.-H.; Hoffmann, G.; Wiesendanger, R.; Lensen, R.; Kouwer, P. H. J.; et al. Dynamics of Molecular Self-Ordering in Tetraphenyl Porphyrin Monolayers on Metallic Substrates. *Nanotechnology* **2009**, *20*, 275602/1–275602/10.

(33) Buchner, F.; Kellner, I.; Hieringer, W.; Görling, A.; Steinrück, H.-P.; Marbach, H. Ordering Aspects and Intramolecular Conformation of Tetraphenylporphyrins on Ag(111). *Phys. Chem. Chem. Phys.* **2010**, *12*, 13082–13090.

(34) Duhm, S.; Gerlach, A.; Salzmann, I.; Bröcker, B.; Johnson, R.; Schreiber, F.; Koch, N. PTCDA on Au(111), Ag(111) and Cu(111): Correlating Bonding Distance and Interfacial Charge Transfer. *Org. Electron.* **2008**, *9*, 111–118.

(35) Bürker, C.; Ferri, N.; Tkatchenko, A.; Gerlach, A.; Niederhausen, J.; Hosokai, T.; Duhm, S.; Zegenhagen, J.; Koch, N.; Schreiber, F. Exploring the Bonding of Large Hydrocarbons on Noble Metals: Diindoperylene on Cu(111), Ag(111), and Au(111). *Phys. Rev. B* **2013**, *87*, 165443/1–165443/5.

(36) Stadtmüller, B.; Kröger, I.; Reinert, F.; Kumpf, C. Submonolayer Growth of CuPc on Noble Metal Surfaces. *Phys. Rev. B* **2011**, *83*, 085416/1–085416/10.

(37) Hauschild, A.; Karki, K.; Cowie, B. C. C.; Rohlfing, M.; Tautz, F. S.; Sokolowski, M. Molecular Distortions and Chemical Bonding of a Large  $\pi$ -Conjugated Molecule on a Metal Surface. *Phys. Rev. Lett.* **2005**, *94*, 036106/1–036106/4.

(38) Gerlach, A.; Hosokai, T.; Duhm, S.; Kera, S.; Hofmann, O. T.; Zojer, E.; Zegenhagen, J.; Schreiber, F. Orientational Ordering of Nonplanar Phthalocyanines on Cu(111): Strength and Orientation of the Electric Dipole Moment. *Phys. Rev. Lett.* **2011**, *106*, 156102/1–156102/4.

(39) Henze, S. K. M.; Bauer, O.; Lee, T.-L.; Sokolowski, M.; Tautz, F. S. Vertical Bonding Distances of PTCDA on Au(111) and Ag(111): Relation to the Bonding Type. *Surf. Sci.* **2007**, *601*, 1566–1573.

(40) Kilian, L.; Hauschild, A.; Temirov, R.; Soubatch, S.; Schöll, A.; Bendounan, A.; Reinert, F.; Lee, T.-L.; Tautz, F. S.; Sokolowski, M.; et al. Role of Intermolecular Interactions on the Electronic and Geometric Structure of a Large  $\pi$ -Conjugated Molecule Adsorbed on a Metal Surface. *Phys. Rev. Lett.* **2008**, *100*, 136103/1–136103/4.

(41) Gerlach, A.; Bürker, C.; Hosokai, T.; Schreiber, F. In *The Molecule–Metal Interface*; Koch, N., Ueno, N., Wee, A., Eds.; WILEY–VCH Verlag: New York, 2013.

(42) Zegenhagen, J. Surface-Structure Determination with X-ray Standing Waves. *Surf. Sci. Rep.* **1993**, *18*, 199–271.

(43) Woodruff, D. P.; Seymour, D. L.; McConville, C. F.; Riley, C. E.; Crapper, M. D.; Prince, N.; Jones, R. G. A Simple X-ray Standing Wave Technique for Surface Structure Determination — Theory and an Application. *Surf. Sci.* **1988**, *195*, 237–254.

(44) Cheng, L.; Fenter, P.; Bedzyk, M. J.; Sturchio, N. C. Fourier-Expansion Solution of Atom Distributions in a Crystal Using X-ray Standing Waves. *Phys. Rev. Lett.* **2003**, *90*, 255503/1–255503/4.

(45) Touloukian, Y. S.; Kirby, R. K.; Taylor, R. E.; Desai, P. D. *Thermophysical Properties of Matter. Vol. 12: Thermal Expansion - Metallic Elements and Alloys*; IFI Plenum: New York, Washington, DC, 1975.

(46) See the Supporting Information. It contains the desorption spectrum of a CuTPP monolayer, the details of the metalation reaction due to hard X-rays exposure, and the details of the calculation of the bending angles for the phenyl groups.

(47) Buchner, F.; Zillner, E.; Röckert, M.; Gläsel, S.; Steinrück, H.-P.; Marbach, H. Substrate-Mediated Phase Separation of Two Porphyrin Derivatives on Cu(111). *Chem.—Eur. J.* **2011**, *17*, 10226–10229.

(48) Di Santo, G.; Blankenburg, S.; Castellarin-Cudia, C.; Fanetti, M.; Borghetti, P.; Sangaletti, L.; Floreano, L.; Verdini, A.; Magnano, E.; Bondino, F.; et al. Supramolecular Engineering through Temperature-Induced Chemical Modification of 2H-Tetraphenylporphyrin on Ag(111): Flat Phenyl Conformation and Possible Dehydrogenation Reactions. *Chem.—Eur. J.* **2011**, *17*, 14354–14359.

(49) Kröger, I.; Bayersdorfer, P.; Stadtmüller, B.; Kleimann, C.; Mercurio, G.; Reinert, F.; Kumpf, C. Submonolayer Growth of H<sub>2</sub>-Phthalocyanine on Ag(111). *Phys. Rev. B* **2012**, *86*, 195412/1–195412/9.

(50) Duhm, S.; Bürker, C.; Niederhausen, J.; Salzmann, I.; Hosokai, T.; Duvernay, J.; Kera, S.; Schreiber, F.; Koch, N.; Ueno, N.; et al. Pentacene on Ag(111): Correlation of Bonding Distance with Intermolecular Interaction and Order. *ACS Appl. Mater. Interfaces* **2013**, *5*, 9377–9381.

(51) Kröger, I.; Stadtmüller, B.; Kleimann, C.; Rajput, P.; Kumpf, C. Normal-Incidence X-ray Standing-Wave Study of Copper Phthalocyanine Submonolayers on Cu(111) and Au(111). *Phys. Rev. B* **2011**, *83*, 195414/1–195414/9.